nature climate change

SUPPLEMENTARY INFORMATION

DOI: 10.1038/NCLIMATE1659

Disease and thermal acclimation in a more variable and unpredictable climate

T. R. Raffel *et al.*

Supplementary Methods

Modeling methods:

We used a mathematical model to describe how the timescale and predictability of temperature variation should interact to influence the geometric population growth rate (G) of a microparasite within a host, assuming the same level of parasite exposure for all hosts. In this model, we explored the consequences of differential rates of parasite and host acclimation for parasite population growth, assuming that both parasite infectivity and host resistance increase with time following a temperature shift. In the context of this model, parasite infectivity (I) refers to the geometric population growth rate of a microparasite in the absence of host resistance, and host resistance (R) refers to the effectiveness of the host immune system and/or behavioral avoidance mechanisms at reducing parasitic growth. R is bound between 0 (completely ineffective at reducing parasitic growth) and 1 (completely resistant to infection). I is constrained to be greater than 0, and $I > 1$ indicates positive population growth of a microparasite when $R = 0$. Parasite population growth is then modeled as a function of parasite infectivity and host resistance such that:

$$G = I - (I \times R) \qquad (1)$$

Rather than model temperature effects explicitly, we made the simplifying assumption that parasite infectivity or host resistance each starts at some low "unacclimated" level following any unpredictable temperature shift, and then gradually increases to a higher "acclimated" level given sufficient time at the new temperature (Supplementary Fig. 1a). We modeled the increase in infectivity and resistance through time ($I = i\{t\}$ and $R = r\{t\}$) as logistic functions starting at low initial values (i_0 and r_0) and approaching higher levels as acclimation time grows large ($i\{t_\infty\}$ or $r\{t_\infty\}$). Each logistic curve has two parameters, the half-saturation point M (the time at which infectivity or resistance is half-way to being fully acclimated) and rate constant λ, which controls the degree of curvature. We used $\lambda = 6$ in all simulations.

$$i\{t\} = i\{t_0\} + \frac{i\{t_\infty\} - i\{t_0\}}{1 + e^{\left(\frac{-\lambda(t-M_i)}{M_i}\right)}} \qquad (2)$$

$$r\{t\} = r\{t_0\} + \frac{r\{t_\infty\} - r\{t_0\}}{1 + e^{\left(\frac{-\lambda(t-M_r)}{M_r}\right)}} \qquad (3)$$

Given that many organisms can anticipate and acclimate to predictable diurnal and seasonal fluctuations[17, 28], we modeled the effect of predictability (or "banality") by adding a parameter (B) to represent the probability that temperature can be correctly predicted by an organism. We assumed that perfect predictability of temperature variation ($B = 1$) allows organisms to anticipate a new temperature perfectly, such that parasite infectivity and host resistance would be acclimated with no time lag following a temperature shift (i.e., $i\{t_0\} = i\{t_\infty\}$ and $r\{t_0\} = r\{t_\infty\}$). At lower levels of predictability, we assumed that the degree of initial acclimation would be linearly related to B (Supplementary Fig. 1b) such that:

$$i\{t_0\} = i_0 + B * [i\{t_\infty\} - i_0] \qquad (4)$$

$$r\{t_0\} = r_0 + B * [r\{t_\infty\} - r_0] \qquad (5)$$

We combined these equations to estimate the instantaneous population growth rate of a microparasite (i.e., the parasite growth rate at any given time point following a temperature shift, assuming constant exposure) using a modification of eq. 1 (Supplementary Fig. 1c):

$$g\{t\} = i\{t\} - [i\{t\} \times r\{t\}] \qquad (6)$$

To predict the outcome of an infection process that occurs over an extended time period (e.g., 14 or 28 days of *Bd* growth on frogs), we then calculated the cumulative average parasite growth on a host since the time of the temperature shift. This value also provides an indication of average parasite growth on a host through time, in an environment where temperature shifts occur with frequency $1/t$, i.e., where t is the average time between temperature shifts (Supplementary Fig. 1d).

$$G\{t\} = \frac{1}{t} \times \sum_{j=1}^{t} g\{t_j\} \qquad (7)$$

Because this framework does not model temperature explicitly, it does not incorporate effects of the amplitude of temperature shifts, nor does it account for possible differences in acclimation ability at different temperatures. Greater magnitude temperature shifts are likely to increase the need for acclimation responses, which would tend to magnify the predicted effects

of this model. Temperature-explicit models would be necessary to predict effects of temperature variability in particular parasite-host systems.

Modeling effects of predictability and timescale on amphibian *Bd* infection:

The effects of time scale in this model are independent of the time unit used, so long as time is considered relative to the half-saturation times for parasite and host acclimation, M_r and M_i. Therefore, the behaviour of the model depends on the relative magnitude of M_r vs. M_i, more so than the absolute values of these parameters. Frog immune system acclimation probably takes on the order of 1-5 weeks based on findings for other ectothermic vertebrates[19], but the acclimation time for *Bd* infectivity remains unknown. We therefore used metabolic theory to estimate plausible acclimation times for *Bd* infectivity and frog anti-*Bd* resistance.

Gillooly et al.[20] showed that organism mass can be used to predict the time it takes for biological processes to occur, such that:

$$t_b \propto (Mass)^{1/4} e^{E_i/kT} \qquad (8),$$

where t_b is the biological process time, E_i is the activation energy for the process, k is Boltzmann's constant, and T is the temperature in degrees Kelvin. This equation predicted life-span over a wide range of fish and invertebrate body masses, and the underlying relationship between body size and metabolic rate holds for organisms ranging from vertebrates to unicellular organisms[20]. Therefore, we postulated that acclimation times of parasites and hosts would also be proportional to $(Mass)^{1/4}$. Assuming similar activation energies for host and parasite, this means that the ratio of host to parasite acclimation times should be proportional to the quarter power of the ratio of host to parasite masses.

Infected frogs in Experiment 1 had an average mass of 1.2 g, and *Bd* zoospores have an approximate diameter of 40 μm[23] for a mass of approximately 3.4×10^{-8} g. This means that the host-to-parasite mass ratio was approximately 3.6×10^{7}. The quarter power of 3.6×10^{7} is 77, so we postulated that frog acclimation time is at least 10 times longer than parasite acclimation time and used a conservative estimate of $M_r/M_i = 10$. To provide intuitive model outputs on the time scale of the experiments, we set $M_r = 10$ days in model simulations as an educated guess for the number of days it takes for the frog immune system to become half-acclimated. However, the model results were qualitatively robust to the values of M_r and M_i, so long as $M_r > M_i$.

To generate the graphs for Figure 1, we used M_i=1, M_r=10, i_0=1, r_0=0.2, λ=6, and $i\{t_\infty\}$=3, with $r\{t_\infty\}$=0.9 in Fig. 1a and $r\{t_\infty\}$=0.5 in Fig. 1b. Model outputs and graphics were generated using R statistical software[31].

Animal collection and maintenance:

Adult Cuban treefrogs (*Osteopilus septentrionalis*) were collected from Hillsborough County, FL within one month of the start the first acclimation experiment and the diurnal temperature experiment. For *Acclimation Experiment 2*, recently metamorphosed frogs were obtained by filling wading pools and cattle watering tanks and leaving them open at the University of South Florida (USF) Botanical Gardens, allowing colonization by algae and Cuban treefrogs. Several breeding pairs of Cuban treefrogs laid eggs in these pools. Tadpoles were allowed to develop and were collected as they metamorphosed. Once collected, frogs were maintained in 1 L deli cups with air holes and wet paper towels. They were provided clean towels and vitamin-dusted crickets weekly until the start of each experiment.

Experimental incubators:

We manipulated temperature for each replicate using a customized Styrofoam incubator (inner dimensions 37x21x13 cm; Marko Foam Products, Salt Lake City, UT), each with temperature individually maintained by heat tape (Flexwatt Industrial Sales, Maryville, TN) controlled by a bulb-and-capillary thermostat (Selco Products Co., Orange, CA). Each incubator had a double-pane plexiglass window in the lid to provide light, and a folded towel to buffer frogs from the heat tape (Supplementary Fig. 2). Incubators were arranged on shelves in a GR48 environmental chamber (Environmental Growth Chambers, Chagrin Falls, OH) set to approximately 15°C. "Cold" incubators (target 15°C) were maintained at the ambient temperature, whereas "warm" (25°C) or "medium" (20°C) incubators were calibrated to maintain the target temperature. Positions of the frogs' individual containers were shuffled daily within each incubator to control for possible effects of position on temperature or light. Variable temperatures (Diurnal temperature, DT; Random temperature, RT) were attained by calibrating incubators to 25°C and turning the incubators on or off, either with a timer set to a 12/12 day/night cycle (DT) or by plugging or unplugging incubators each day based on a randomization schedule (RT).

Actual temperatures:

Actual temperatures within incubators were recorded during experiments using 20 Hobo pendant temperature/light data loggers (Onset Computer Corporation, Pocasset, MA). Incubators found to be more than 1°C above or below the target temperature were adjusted to improve calibration. The cold room temperature was checked daily for the entirety of each experiment, and room temperatures were recorded during the exposure period of *Acclimation Experiment 1* and during all of the *Diurnal Temperature Experiment* and *Acclimation Experiment 2* (Supplementary Fig. 4a-c).

For *Acclimation Experiment 1*, "warm" incubators (target temperature 25°C) were calibrated prior to the start of the experiment and temperatures were measured again two days prior to the temperature shift, during the acclimation period. The average temperature at this time was approximately 2°C below the target temperature of 25°C (Supplementary Fig. 4d). Therefore, all available loggers were devoted to recalibrating the warm (25°C) incubators during this period, and estimates of actual acclimation temperatures for the 15°C treatment were derived from data collected just before the start of the acclimation period (Supplementary Fig. 4e). During the exposure period, temperature data were collected on 3-4 dates for each incubator, and actual temperatures of warm incubators during this period were maintained within 2°C of the target temperature (Supplementary Fig. 4e). The "cold" incubators (target temperature 15°C) were approximately 1°C lower than the target temperature throughout the experiment (Supplementary Fig. 4c).

For the *Diurnal Temperature Experiment* and *Acclimation Experiment 2*, incubators were calibrated using Coralife® digital aquarium thermometers (Central Garden & Pet Company, Walnut Creek, CA). Temperature loggers were cycled through the incubators so that data were collected for each incubator on every fourth day. Actual mean temperatures were maintained within 3°C of the target temperatures, with most incubators remaining within 1.5°C of the target throughout each experiment (Supplementary Fig. 4e, f). Both of the variable-temperature treatments in the *Diurnal Temperature Experiment* had an average standard deviation of approximately 5°C (Supplementary Fig. 4f, g). Diurnal temperature shifts were more abrupt than would typically be observed in nature, shifting from one temperature to the other over the course of 1-2 hours rather than in a continuous sinusoidal curve (Supplementary Fig. 4h).

Experimental conditions:

Replication of temperature treatments was achieved by using individual custom-built incubators placed in an environmental chamber set on a 12 hr light cycle (Supplementary Fig. 2). Within each incubator, frogs were maintained individually in vented plastic containers (350 mL in the Acclimation experiments; 700 mL in the *Diurnal Temperature Experiment*). In *Acclimation Experiment 1* and the *Diurnal Temperature Experiment*, frogs were maintained on autoclaved soil (125 mL per container) collected from the USF Botanical Gardens and kept wet by adding deionized water as needed. Soil was changed every two weeks. In the second acclimation experiment, two tri-fold towels soaked with 20 mL of artificial spring water were used as substrate instead of soil and were changed once per week. In all three experiments, frogs were fed 5-10 crickets (5-15 mm) once per week. The Acclimation experiments each had two temporal blocks and the *Diurnal Temperature Experiment* had eight spatial blocks, with temperature treatments randomly assigned within each block.

Bd inoculation and cultures:

Previous studies of temperature effects on *Bd* growth in culture have used a single inoculate for cultures at all temperatures[22,27,32]. In these studies, the inoculate culture was grown at or above 23°C (the accepted optimum temperature for growth) prior to inoculation[22,27]. In this study, however, it was critical that the *Bd* inoculate be acclimated to the exposure temperature prior to inoculation, ensuring that temperature-shift effects on *Bd* growth on frogs could only be caused by changes in frog resistance. If *Bd* inoculates were also shifted in temperature at the time of exposure, the effects of frog acclimation could have been confounded with acclimation effects on *Bd* itself. For example, *Bd* zoospore production increased following a temperature shift from 26.5°C to 7.0°C[22]. We therefore used a separate inoculate for each exposure temperature for the *Acclimation* and *Diurnal Temperature* experiments, acclimating each inoculate to the exposure temperature for a week prior to inoculation.

The *Bd* strain used in this study (SRS 812) was originally cultured from a bullfrog tadpole at the Savannah River Site, SC, USA in August 2006 and has since been maintained in culture at 4°C. *Bd* inoculates were grown in 1% tryptone broth. Inoculates for frog exposures were passed through a 20 μm nylon filter (Spectrum Laboratories, Inc., Rancho Dominguez, CA) to isolate infective zoospores. Each frog was exposed by pipetting 10^6 zoospores in 3 mL (*Acclimation Experiment 1* and *Diurnal Temperature Experiment*) or 2 mL (*Acclimation*

Experiment 2) of tryptone broth onto the frog's skin. Excess broth was allowed to trickle into the frog's container. Assuming both frogs in a given incubator survived to the end of the acclimation period, the second frog was treated similarly with the same volume of sterile broth as a control. The vinyl gloves used to handle frogs were rinsed with 70% ethanol and dried before moving to the next frog.

In *Acclimation Experiment 1* and the *Diurnal Temperature Experiment*, each incubator also contained a sealed broth *Bd* culture (8.5 mL and 5.1 mL, respectively). Zoosporangia contribute more to growth in new cultures than zoospores[23], so culture inoculates were left unfiltered and diluted to standardize initial zoosporangium densities across each temporal block (*Acclimation Experiment 1*, Block 1: 4.6×10^3 mL^{-1}, Block 2: 2.4×10^3 mL^{-1}; *Diurnal Temperature Experiment*: 1.0×10^3 mL^{-1}). Zoosporagium density was measured using a compound microscope and hemocytometer, and *Bd* growth was quantified as the proportional increase in zoosporangium density seven days post-inoculation.

To determine whether the *Bd* strain used in this study (SRS 812) has similar temperature-dependent growth compared to previously studied *Bd* strains, we conducted an additional *Bd* culture experiment to obtain a temperature-dependent growth curve. To more closely replicate conditions used in previous studies of temperature-dependent *Bd* growth (e.g., Piotrowski et al.[32]), we used a single inoculate which had been acclimated to 23°C, and we measured *Bd* growth as changes in optical density (absorbance at 490 nm) rather than using counts of zoosporangia. We measured *Bd* growth in replicate incubators set to 10, 15, 20, 25, or 30°C (N = 3 incubators per temperature). All incubators had actual temperatures within ±1°C of the target temperature. Each incubator contained a 1% tryptone broth culture of *Bd* (*Bd*+ culture: 3.6×10^5 zoospores in 6.0 mL of broth) and a second tube containing sterile broth (*Bd*- culture). The absorbance of a 100 µL aliquot from each culture was taken on days 0, 4, 8, and 12 of the experiment. Temperature affected broth absorbance, so to control for this we subtracted the absorbance of the *Bd*- culture from the *Bd*+ culture in each incubator. We calculated the *Bd* population growth rate per day (r) for each culture from the slope of the relationship between log-transformed absorbance and time. There was evidence of density-dependent growth at Day 12, so we omitted this time point from the analysis. We then fit a third-order polynomial function to these population growth rates, constraining the curve to pass through the origin ($r = 0$ at 0°C). Under these conditions, the *Bd* growth curve was similar to published growth curves for other *Bd* strains (Supplementary Fig. 5)[22,27,32].

Swabbing and quantitative PCR details:

Bd growth on frogs was measured by swabbing each frog at two and four weeks post-exposure or on the day a frog died. The number of *Bd* genome equivalents on each swab was measured using quantitative PCR. The swab was passed over the underside of each hindlimb and frozen for later processing. For *Acclimation Experiment 1* and the *Diurnal Temperature Experiment*, the swab was passed 10 times from hip to knee and 15 times from ankle to toe of each hindlimb. For *Acclimation Experiment 2*, the swab was passed 5 times from hip to knee and 5 times from ankle to toe for each hindlimb. To prevent cross-contamination with *Bd* DNA, the vinyl gloves used to handle each frog were rinsed sequentially in 10% bleach, 1% Novaqua® to neutralize the bleach, and deionized water before swabbing the next frog.

DNA was extracted using 40 μL Prepman Ultra, and PCR reactions were run with a StepOne™ Real-Time PCR System (Applied Biosystems, Foster City, CA), using the procedure described by Kriger et al.[33]. Test samples were run in singlicate to control costs, as recommended by Kriger et al.[33]. We added TaqMan® Exogenous Internal Positive Control (Exo IPC) Reagents (Applied Biosystems, Foster City, CA) to every reaction well to assess inhibition of the PCR reaction[33], which can be caused by soil contamination. In this Exo IPC system, a standardized concentration of an artificial DNA sequence is added to each reaction well with its own set of primers and a separate fluorescent probe, and the strength of this reaction is used to assess overall reaction inhibition. Samples in *Acclimation Experiment 1* were first analyzed at 1:10 dilution and judged inhibited if the C_T score of the Exo IPC reaction was more than 6.0 greater than the average C_T score of the negative control wells (53% of *Bd*-exposed samples, evenly distributed across treatment groups). These samples were re-run with a further 1:10 dilution (to 1:100), and two samples required one more dilution step (1:1000) to remove inhibition. For *Acclimation Experiment 2* and the *Diurnal Temperature Experiment*, all samples were analyzed initially with the 1:100 dilution and inhibited samples (*Acclimation Experiment 2*: 1.3% of samples; *Diurnal Temperature Experiment*: 11% of samples) were re-run with a 1:1000 dilution to remove inhibition.

Monthly climate variability and neotropical frog declines:

Rohr and Raffel[6] reanalyzed the last year observed (LYO) and year of decline (YOD) datasets, which describe the timing of the decline of 68 frog species in genus *Atelopus* between 1980-1998. They found that the absolute value of monthly differences in temperature (AVMD)

and diurnal temperature range (DTR) were the best climatic predictors of these *Bd*-related declines[6]. Briefly, they obtained climate data from the Climate Research Unit (CRU TS 2.1), University of East Anglia for the region inhabited by *Atelopus* spp.[27], and calculated AVMD by subtracting the mean temperatures for adjacent months, taking the absolute values of these differences, and averaging these differences for each year[6]. DTR was the mean difference between daily minimum and maximum temperatures for each year. The proportions of species disappearing or declining each year for each dataset (LYO or YOD) were angularly transformed and then detrended using generalized additive models (GAM), to control for possible temporal confoundment. Best subsets regression was used to choose the best predictors of LYO and YOD. The best models included 1-year lags between predictors and response variables except for the effect of AVMD on YOD. DTR changed nonlinearly with time and was therefore analyzed with and without GAM detrending.

To test whether the previously discovered relationship between monthly temperature variability and *Atelopus* spp. declines was caused more by monthly increases or decreases in temperature, we re-conducted the original model fitting using these two new predictor variables. Monthly increases and decreases in temperature were calculated by including only monthly differences that were positive or negative, respectively. As before, we conducted these analyses with and without DTR as a covariate, and with or without detrending DTR. Models were compared using Akaike's information criterion (AIC_c), and the contributions of predictors to individual models were assessed using F-tests.

Are diurnal temperature effects in Latin America actually due to daily minima or maxima?

Diurnal temperature range was a positive predictor of *Bd*-related frog declines in Latin America[6]. One possible explanation of this relationship is that years with wider diurnal temperature ranges were also years with lower nighttime temperatures, which might make frogs more susceptible to *Bd* infection (Fig. 2, 3). To assess relationships between daily minimum temperatures (T_{min}), daily maximum temperatures (T_{max}), and diurnal temperature range (DTR) at individual locations in South America, we obtained daily temperature data from the National Climatic Data Center (Surface data: Global summary of the day. National Climatic Data Center, Asheville, NC. http://www7.ncdc.noaa.gov/CDO/cdo. Data for 1/1/1980-12/1/2004. Accessed 1/3/2011). We selected stations within the South America geographic region with date ranges from 1/1/1980 to 12/1/2004, starting alphabetically at "Abrolhos" and continuing to

"Ibague/Perales". This yielded 144 stations distributed throughout South America. For each station, we calculated the average daily minimum temperature (T_{min},), daily maximum temperature (T_{max}) and diurnal temperature range (DTR, i.e. $T_{min} - T_{max}$) for each year with at least 150 days of complete data. We then narrowed the dataset further to include only those stations with at least 15 years of data (>150 days' worth of data per year) that were located within the geographic limits of -57° to -80° longitude and -20 to 20 degrees latitude. This resulted in a final total of 31 stations (Supplementary Table 8). We then calculated Pearson correlation coefficients for each station to describe the relationships between T_{min} & DTR and between T_{max} & DTR (Supplementary Table 8, Supplementary Fig. 6).

Statistical analysis details:

All analyses were conducted using R statistical software[31]. The functions and packages we used are listed in Supplementary Table 9. *Bd* growth in culture was analyzed using generalized linear models (glzm) with gamma errors. Frog survival was analyzed with censored survival regression using the extreme value distribution, which allows the rate of mortality to vary with time (survival analyses using the Weibull distribution or Cox proportional hazards produced similar results). All P-values were calculated using two-tailed tests.

Frog *Bd* infection (zoospore genome equivalents, GE) was analyzed using zero-inflated negative binomial glzm. Zero-inflated models assume that the response variable is a function of a binomial process (uninfected vs. infected) and a count process (negative-binomial distributed infection intensity)[34]. In these models, zeros (apparently uninfected frogs) can arise from either process (i.e., true negatives or false positives). We used a simplified version of zero-inflated models in which the binomial component of the model is constrained to have a single parameter. Treatment effects were assessed with likelihood ratio tests, using a Type II sums of squares procedure to avoid inappropriate removal of marginal terms from models[35]. Each frog was swabbed twice, so it would have been appropriate to analyze the *Bd* infection data as a repeated measures design (i.e., using a mixed-effects model). However, many frogs died prior to Week 4 post-infection, particularly in the 15°C and 20°C temperature treatments, so that these frogs had less time for *Bd* to grow on them. This makes the Week 4 data less straightforward to interpret than the Week 2 data. We therefore analyzed the Week 2 and Week 4 swab data separately, and we focused on swabs taken from live frogs at Week 2 post-infection to avoid death as a potentially confounding factor. For the analysis of *Bd* load in the Week 4 time period, we

included all swabs from frogs surviving until at least 23 days post-exposure to avoid a missing-cells design.

For the *Acclimation* experiments, we tested for effects of *Bd* exposure, exposure temperature, and acclimation. Both experiments were run in two temporal blocks to make them more manageable, so we included temporal block as a factor in all analyses of these experiments. For the *Diurnal Temperature* experiment, we tested for overall effects of *Bd* exposure and temperature treatment. This experiment had eight spatial blocks rather than temporal blocks, so we including spatial block as a factor for all analyses of this experiment. We then conducted multiple comparisons among the five treatment levels (15°C, 20°C, 25°C, Diurnal and Random), adjusting P-values to control for a false discovery rate of 0.05[36], using the "mt.rawp2adjp" function in the "multtest" package of R statistical software. Frog mass was included as a covariate in all primary analyses (Supplementary Tables 2, 4, & 5). Mass was retained as a covariate in secondary analyses (Supplementary Table 3 and multiple-comparisons tests) if it contributed significantly to the primary analysis.

Supplementary Notes and Discussion

Modeling Outputs:

Certain features of the model were true for all parameter values. At very short timescales ($t \to 0$), neither parasite nor host has time to acclimate, so the parasite population growth rate approaches $G\{t_0\} \approx g\{t_0\} \approx i\{t_0\} - (i\{t_0\} \times r\{t_0\})$. On very long timescales ($t \to \infty$) or high levels of predictability ($B \to 1$), both host and parasite are nearly perfectly acclimated and parasite growth approaches an equilibrium value of $G\{t_\infty\} \approx g\{t_\infty\} \approx i\{t_\infty\} - (i\{t_\infty\} \times r\{t_\infty\})$.

If we assume that acclimation time for parasite infectivity is shorter than for host resistance ($M_i < M_r$), as argued above, then parasite growth is always highest at intermediate time scales unless the parasite has no acclimation response ($i\{t_\infty\} = i\{t_0\}$; Supplementary Fig. 1c, d). This is because growth increases with time since a temperature shift until the parasite fully acclimates to the new temperature, followed by decreasing parasite growth rate with time as the host continues to acclimate (Supplementary Fig. 1c, d). The timing of peak parasite growth depends on the relative values of M_i and M_r., occurring earlier for smaller values of M_i. The magnitude of peak parasite growth and the subsequent rate of decrease in parasite growth with increasing time scale depended on the relative acclimation abilities of parasite and host ($i\{t_\infty\}$

and $r\{t_\infty\}$), with higher peaks and equilibrium values for $s\{t\}$ and $S\{t\}$ when $i\{t_\infty\}$ is large relative to $r\{t_\infty\}$ (Fig. 1; Supplementary Fig. 1c, d).

The effect of predictability in temperature on parasite growth depended on the relative acclimation abilities of parasite and host ($i\{t_\infty\}$ and $r\{t_\infty\}$). Greater predictability gives benefits the host if $r\{t_\infty\}$ is large relative to $i\{t_\infty\}$ (Fig. 1a), whereas predictability benefits the parasite if $i\{t_\infty\}$ is large relative to $r\{t_\infty\}$ (Fig. 1b).

Mortality due to *Bd* infection and testing controls for *Bd*:

We included control frogs in each experiment to test whether mortality patterns in the *Bd*-exposure were caused by infection and not by main effects of temperature on host vigor. We observed significant mortality due to *Bd* exposure in all three experiments (Supplementary Fig. 6, Supplementary Tables 4 & 5), with low levels of control mortality (Supplementary Fig. 7). We also tested control frogs for *Bd* infection using qPCR. None of the control frogs in *Acclimation Experiment 1* had detectable levels of *Bd* infection, but some in *Acclimation Experiment 2* and the *Diurnal Temperature Experiment* appear to have been infected with *Bd* (13/39 and 11/61 infected, respectively). However, most of these were light infections, well below a previously described threshold for amphibian mortality ≈10,000 zoospore equivalents per swab[37]. Indeed, only six control frogs exceeded 100 zoospore genome equivalents. Given the measures we took to prevent cross-contamination, it seems probable that one or more of these more heavily infected frogs was infected prior to the start of the experiment and served as a source of infection for other control frogs. Four of these frogs died during the exposure period, comprising nearly half of the control mortality in these two experiments. Thus, it appears that the vast majority of mortality in these experiments was indeed caused by *Bd* infection, even in the "control" treatment. Removal of these six infected control frogs from the survival analyses had no qualitative effect on the results.

Differences in *Bd*-induced mortality between Acclimation experiments 1 & 2:

Although the acclimation effects on *Bd* growth were qualitatively similar for the first and second acclimation experiments (Fig. 2a, b), we only observed an acclimation effect on *Bd*-induced mortality in the second experiment (Fig. 2b, c). We cannot be certain what caused this difference because these experiments differed in several respects, though we can speculate about what factors might have caused this discrepancy.

One possible explanation is that the greater variability in size of adult frogs in *Acclimation Experiment 1* increased random variation in *Bd*-induced survival, making it more difficult to distinguish acclimation effects. This difference also helped to account for the greater variance in *Bd* load in *Acclimation Experiment 1* (Fig. 2a, b), in which larger frogs had higher *Bd* loads (Supplementary Table 2). Indeed, *Acclimation Experiment 1* was the only experiment for which inclusion of the mass covariate influenced any of the results, by increasing the significance of the acclimation effect following a temperature decrease (Supplementary Table 3). In contrast, frog size had no apparent effect on *Bd*-induced mortality in *Acclimation Experiment 1* (Supplementary Table 4). These two results together suggest that larger frogs might be more tolerant of infection than smaller frogs, consistent with the previous finding that larger frogs were less likely to die from chytridiomycosis[24]. Such a tolerance effect might have counteracted the effects of higher *Bd* loads on larger frogs, masking size effects on mortality but increasing random variation in mortality due to infection.

Another difference between the two experiments was that both *Bd*-infected and control frogs in *Acclimation Experiment 1* had lower survivorship than in *Acclimation Experiment 2* (Fig. 2c, d; Supplementary Fig. 7). This suggests that frogs in the first experiment were less vigorous than in the second, possibly making it more difficult to detect acclimation effects on mortality.

Ultimately, it is difficult to say whether differences in frog mortality were caused by these or other differences between the two experiments (e.g., time of year, soil substrate vs. paper towels). Further studies will be needed to clarify how context dependencies such as host mass influence acclimation effects on mortality due to infection.

Bd infection four weeks post-exposure:

By four weeks post-exposure, the acclimation effects on *Bd* load were reduced and no longer significant (Supplementary Fig. 8a, b; Supplementary Tables 2 & 3). However, it is difficult to interpret the *Bd* load data at this time point, because we had to include recently dead frogs in this analysis to avoid a missing-cells design. Thus, this analysis was confounded by frog mortality, because *Bd* could no longer increase after a frog died. Hence, the individuals that died early might have had far higher *Bd* loads by Week 4 if they had survived longer, so we cannot determine from these data whether the acclimation effect might have persisted beyond Week 2. We therefore focused on the Week 2 data, which were not confounded by mortality.

Temperature shift frequency cannot explain random vs. diurnal temperature effects:

Although the two variable-temperature treatments had similar means and variances in temperature (see above), they differed in the frequency of temperature shifts, with shifts occurring an average of every 2.18 ± 0.3 (SD) days in the random temperature treatment as compared to every 0.5 days in the diurnal temperature treatment. Thus, treatment effects on *Bd* growth could have been caused by a difference in shift frequency, as an alternative to a difference in shift predictability (as proposed in the main text). Our model predicts that parasite and host acclimation responses will be more effective if temperature shifts occur less frequently. Thus, the frequency hypothesis predicts better parasite and host acclimation responses in the random temperature treatment. In contrast, the predictability hypothesis predicts better parasite and host acclimation responses in the diurnal temperature treatment.

For *Bd* growth in culture, differences in temperature shift frequency should have caused *Bd* to grow faster in the random than the diurnal temperature treatment. We found the opposite pattern (Fig. 3c), contrary to the frequency hypothesis but in support of the predictability hypothesis. For *Bd* growth on frogs, differences in temperature shift frequency should have made frogs more resistant to infection in the random than in the diurnal temperature treatment. However, the results showed that frogs were more resistant to infection in the diurnal temperature treatment (Fig. 3a). Again, this result was contrary to the frequency hypothesis but in support of the predictability hypothesis. Thus we conclude that predictability of temperature shifts is more important than temperature shift frequency at this timescale.

Bd growth and host resistance with random fluctuations vs. constant temperatures:

Our model predicted that unpredictable temperature fluctuations would reduce host resistance to infection, assuming that parasites acclimate more quickly to unpredictable temperature shifts. If this was the case, then frog resistance to *Bd* infection should be lower with random temperature fluctuations than at a constant temperature. To test this hypothesis, we included three constant temperature treatments in the *Diurnal Temperature Experiment*, representing the average (20°C), minimum (15°C), and maximum (25°C) temperatures of the variable temperature treatments.

It was important to include the minimum and maximum temperature treatments in these comparisons, because *Bd* and frogs in the random temperature treatment only experienced the mean temperature for brief periods while transitioning between 15 and 25°C. *Bd* and frogs in the

random temperature treatment spent half their time at 15 and half at 25°C, so the null expectation in the absence of acclimation effects was that *Bd* growth would be intermediate between growth at 15 and 25°C. This intermediate level of growth did not necessarily equal *Bd* growth at the mean temperature (20°C), because temperature had nonlinear effects on *Bd* growth in culture and on frogs (Fig. 3a, b).

Bd growth in culture with random temperature fluctuations was intermediate between growth at 15 and 25°C (Fig. 3a), as expected in the absence of *Bd* acclimation effects. In contrast, *Bd* growth on frogs with random fluctuations was as high as growth at 15°C, which was much higher than growth at 25°C (Fig. 3b). Furthermore, *Bd* growth in culture was significantly higher at constant 20°C than with random fluctuations (Fig. 3a), whereas *Bd* growth on frogs was similar for these treatments (Fig. 3b). These comparisons indicate weaker host resistance with random temperature fluctuations than with constant temperatures, consistent with results from the two acclimation experiments (Fig. 2a, b). This is presumably because frogs cannot acclimate to rapidly fluctuating temperatures.

Potential mechanisms for diurnal temperature association with *Bd*-related amphibian declines:

Rohr and Raffel[6] found higher rates of amphibian declines and apparent extinctions in Central and South America following years with greater diurnal temperature ranges. In this study, we found that frogs exposed to *Bd* with diurnal temperature fluctuations of 15 to 25°C were more, rather than less, resistant to infection than frogs held at a constant mean temperature (Fig. 2b, c). However, this result does not necessarily rule out diurnal temperature range as a driver of amphibian declines. There are several potential explanations for this difference.

First, *Bd* occurrence in frog populations had a non-monotonic relationship with diurnal temperature range, with opposite trends depending on whether diurnal temperature range was relatively high or low[38]. This complex nonlinear relationship between diurnal temperature range and *Bd* might account for differences between experimental and observational studies. Second, the generality of our findings is yet to be tested across multiple amphibian taxa, and there is no guarantee that *Atelopus* spp. frogs possess the same adaptations to diurnal temperature range as Cuban treefrogs. Third, there is evidence that diurnal temperature range has changed in magnitude in recent decades as a result of global climate change[5], and it is possible that this might negatively affect frogs adapted to previous levels of diurnal temperature fluctuations.

Fourth, frog extinctions correlated with the magnitude of the diurnal temperature range in the *Atelopus* spp. dataset, rather than just the presence or absence of diurnal temperature fluctuations as tested in this study. On a local scale in South America, greater diurnal temperature range generally correlates with cooler nighttime temperatures, which might increase *Bd* infection (Supplementary Fig. 6, Supplementary Table 9), though these two parameters were not significantly correlated on the regional scale $P > 0.4$ [6].

Further work will be necessary to assess the generality of our findings to other amphibian species and whether broader diurnal temperature ranges increase susceptibility to *Bd* infection.

31. R Development Core Team. R: A language and environment for statistical computing R Foundation for Statistical Computing, Vienna, Austria. Version 2.8.1. http://www.r-project.org/ (2010).
32. Piotrowski, J. S., Annis, S. L. & Longcore, J. E. Physiology of *Batrachochytrium dendrobatidis*, a chytrid pathogen of amphibians. *Mycologia* **96**, 9-15 (2004).
33. Kriger, K. M., Hines, H. B., Hyatt, A. D., Boyle, D. G. & Hero, J. M. Techniques for detecting chytridiomycosis in wild frogs: comparing histology with real-time Taqman PCR. *Diseases of Aquatic Organisms* **71**, 141-148 (2006).
34. Zeileis, A., Kleiber, C. & Jackman, S. Regression models for count data in R. *J. Stat. Softw.* 27, 1-25 (2008).
35. Langsrud, Y. ANOVA for unbalanced data: Use Type II instead of Type III sums of squares. *Stat. Comput.* **13**, 163-167 (2003).
36. Benjamini, Y. & Hochberg, Y. Controlling the false discovery rate: a practical and powerful approach to multiple testing. *J. Roy. Statist. Soc. Ser. B* 57, 289-300 (1995).
37 Vredenburg, V. T., Knapp, R. A., Tunstall, T. S. & Briggs, C. J. Dynamics of an emerging disease drive large-scale amphibian population extinctions. *Proc. Natl. Acad. Sci USA* **107**, 9689-9694 (2010).
38 Murray, K. A. *et al.* Assessing spatial patterns of disease risk to biodiversity: implications for the management of the amphibian pathogen, *Batrachochytrium dendrobatidis*. *J. Appl. Ecol.* **48**, 163-173 (2011).
39. Therneau, T. & Lumley, T. Package "survival": Survival analysis, including penalised likelihood. R package version 2.34-1. http://CRAN.R-project.org/package=survival (2008).

40. Fox, J. Package “car”: Companion to applied regression R package version 1.2-12. http://www.r-project.org, http://socserv.socsci.mcmaster.ca/jfox/ (2009).
41. Zeileis, A. & Hothorn, T. Diagnostic checking in regression relationships. *R News* 2, 7-10 (2002).
42. Pollard, K. S., Ge, Y., Taylor, S. & Dudoit, S. Package “multtest”: Resampling-based multiple hypothesis testing. R package version 1.23.3. http://www.r-project.org/ (2009).
43. Jackman, S. Package “pscl”: Classes and methods for R developed in the Political Science Computational Laboratory, Stanford University R package version 1.03. http://pscl.stanford.edu/ (2008).
44. Rosseel, Y. lavaan: An R Package for Structural Equation Modeling. *J. Stat. Softw.* 48, 1-36 (2012).

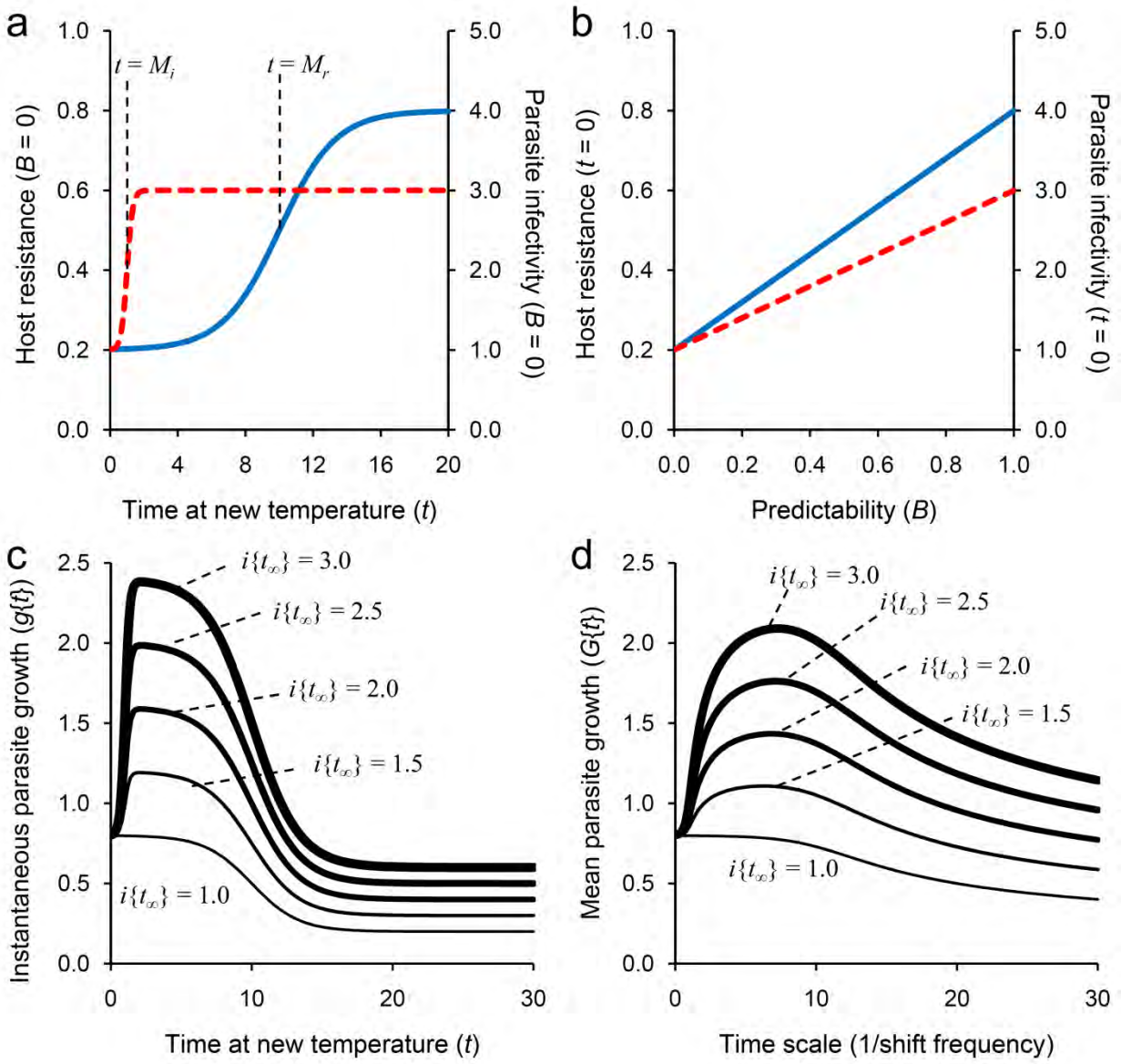

Supplementary Figure S1 | Model predictions for effects of time scale and predictability of temperature variation on parasitism. a, Increases in parasite infectivity (broken red line) and host resistance (solid blue line) with acclimation time (t) following an unpredictable temperature shift ($B = 0$), modeled as a logistic function with $i\{t_\infty\} = 3.0$ and $r\{t_\infty\} = 0.8$. b, Modeled effects of temperature predictability (B) on initial infectivity and resistance ($i\{t_0\}$ and $r\{t_0\}$). c, Changes in the geometric population growth rate of a microparasite ($g\{t\}$) as a function of the time since an unpredictable temperature shift ($B = 0$), for five levels of parasite acclimation ability $i\{t_\infty\}$. d, Changes in mean parasite population growth rate $G\{t\}$ as a function of the mean time between temperature shifts (1/shift frequency), for five levels of parasite acclimation ability $i\{t_\infty\}$ when $B = 0$. Values of $g\{t\} > 1$ or $G\{t\} > 1$ indicate positive parasite population growth. In panels c and d, greater levels of $i\{t_\infty\}$ are indicated by thicker curves. In all panels, $M_i = 1$, $M_r = 10$, $\lambda = 6$, $r\{t_\infty\} = 0.8$, $i_0 = 1.0$, and $r_0 = 0.2$.

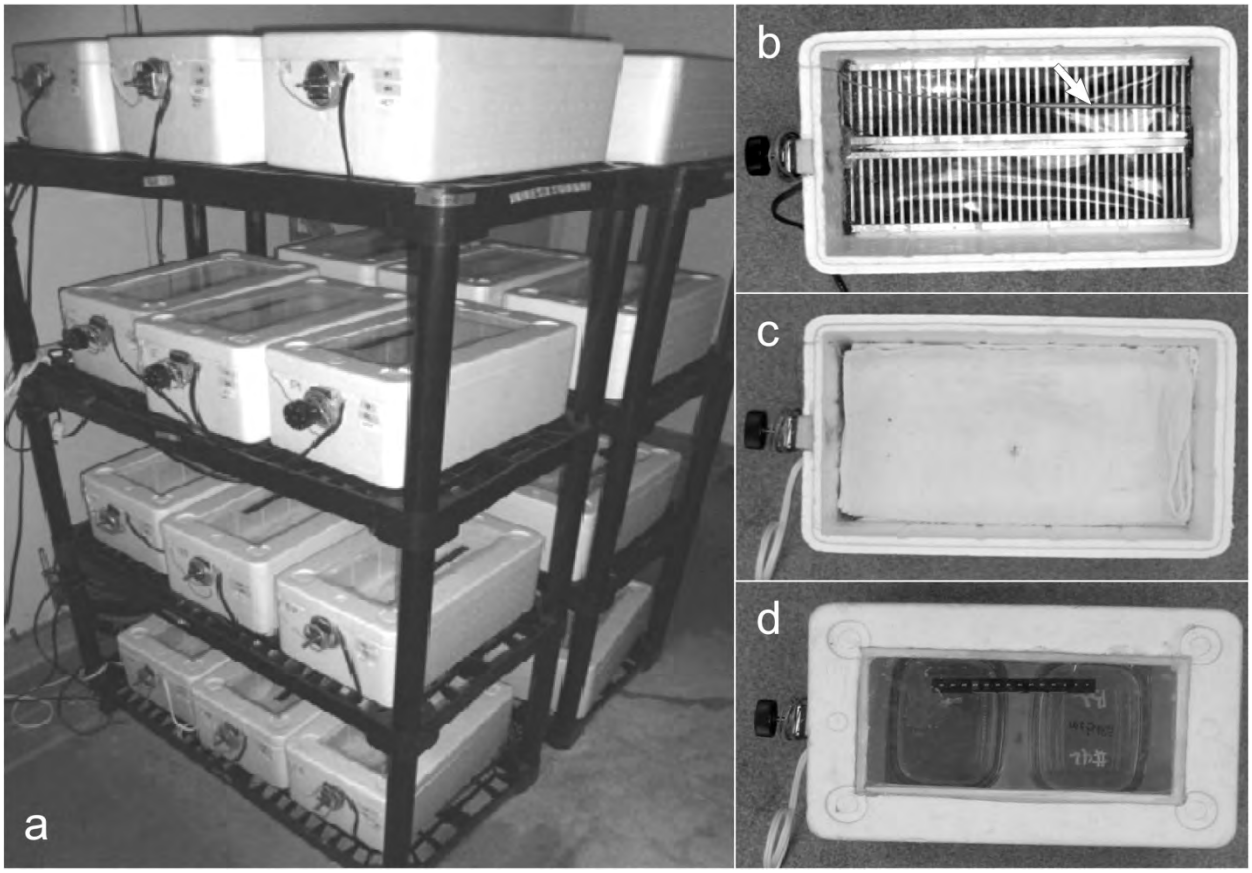

Supplementary Figure S2 | Incubators constructed for replicated controlled-temperature experiments. a, Incubators arrayed on shelving units within the environmental chamber. b, Top view of incubator showing heat tape lining the bottom and the bulb for the bulb-and-capillary thermostat (white arrow). c, Top view of incubator with a towel added to buffer frogs from the heat tape temperatures, folded in three and arranged so the thermostat bulb is under the top layer. d, Top view of complete incubator with lid, containing two frog containers.

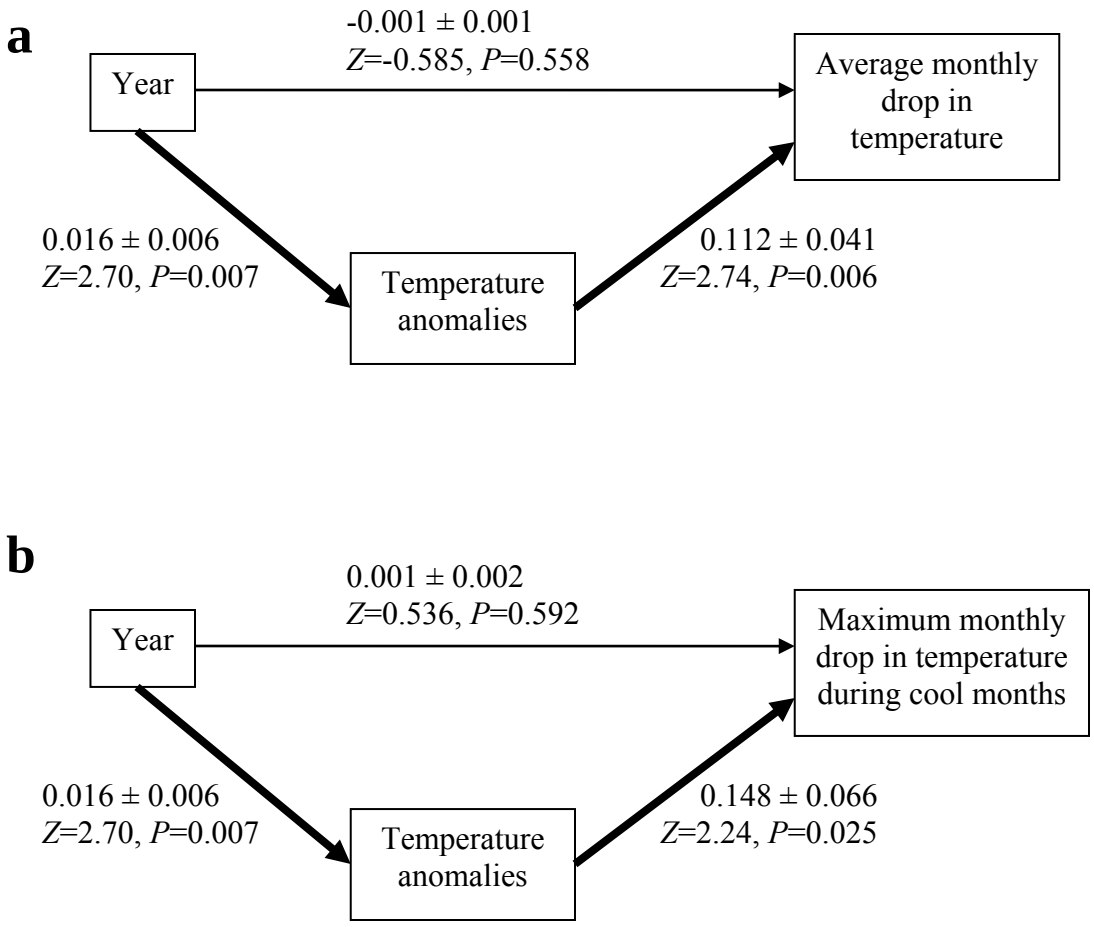

Supplementary Figure S3 | Results of path analyses examining the relationships among year, annual temperature anomalies (i.e. mean temperature), and monthly drops in temperature from 1970-1999. a, monthly drops in temperature represented as average annual monthly drops in temperature. b, monthly drops in temperature represented as the maximum monthly drop in temperature in cool months. Shown next to each arrow are the path coefficient ± standard error, Wald Z statistic, and probability value. Significant paths are bolded. Analyses were conducted using the sem function in the lavaan package of R statistical software.

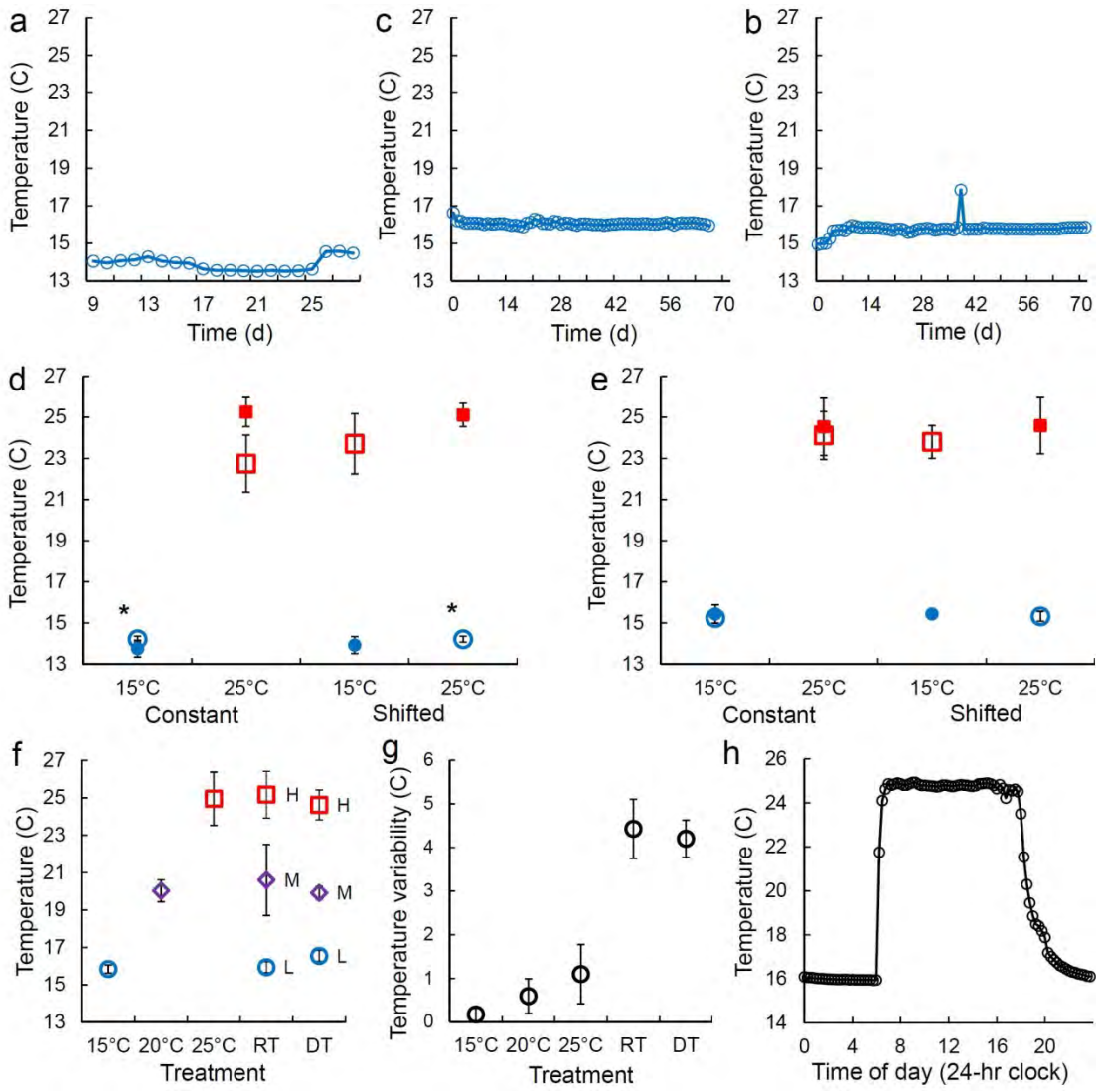

Supplementary Figure S4 | Actual temperatures within incubators. a, External (cold room) temperature during the exposure period of *Acclimation Experiment 1* (Time = days since exposure). b, External temperature during *Acclimation Experiment 2* (Time = days from start of experiment). c, External temperature during the *Diurnal Temperature Experiment* (Time = days from start of experiment). d, Temperatures for *Acclimation Experiment 1* in the four exposure temperature (15 vs. 25°C) by acclimation (Constant vs. Shifted) treatment combinations, measured before (open symbols) and after (closed symbols) the temperature shift (*actual temperatures for cold incubators were measured before the start of this experiment). e, Temperatures for the second acclimation experiment. f, Average temperatures for the *Diurnal Temperature Experiment*, including three constant-temperature treatments and two variable-temperature treatments (RT, Random temperature; DT, Diurnal temperature). For the variable-temperature treatments, average temperatures are presented for periods with high (H) and low (L) target temperatures as well as the overall mean (M) temperature. g, Variability of incubator temperature in the *Diurnal Temperature Experiment*, measured as the standard deviation of incubator temperature. h, Changing temperatures throughout the day for a representative incubator in the diurnal temperature treatment. Target temperature is indicated by symbol color and shape (○ 15°C, ◇ 20°C, □ 25°C). All panels display means ± SD.

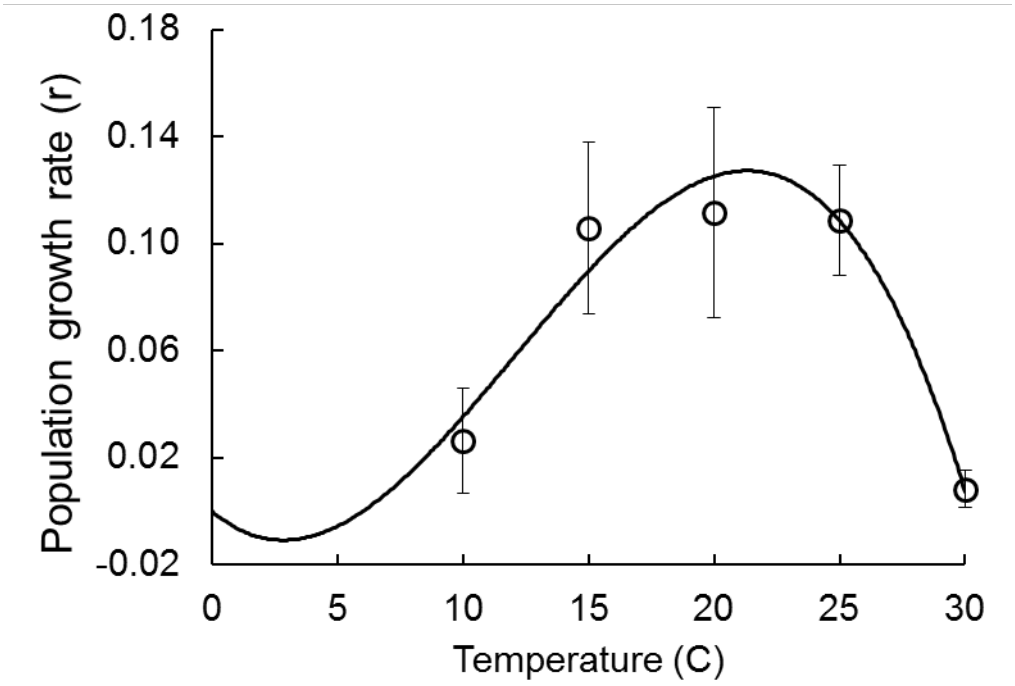

Supplementary Figure S5 | Temperature-dependent population growth rates of *Bd* strain SRS-812 when a single inoculate, acclimated to 23ºC, was used for all temperature treatments. This growth curve is similar to published temperature-dependent growth curves for other *Bd* strains [22,27,32], suggesting that thermal responses of this strain are likely to be representative of *Bd* strains in general. The curve is a third-order polynomial fit to the full dataset ($y = -4.37\times10^{-5}[x^3] + 1.58*10^{-3}[x^2] - 7.91\times10^{-3}[x]$), constrained to pass through the origin (0 growth at 0ºC). Each point represents the average of three replicate cultures, except for the 20ºC point for which one replicate was omitted due to contamination. Error bars ± SE.

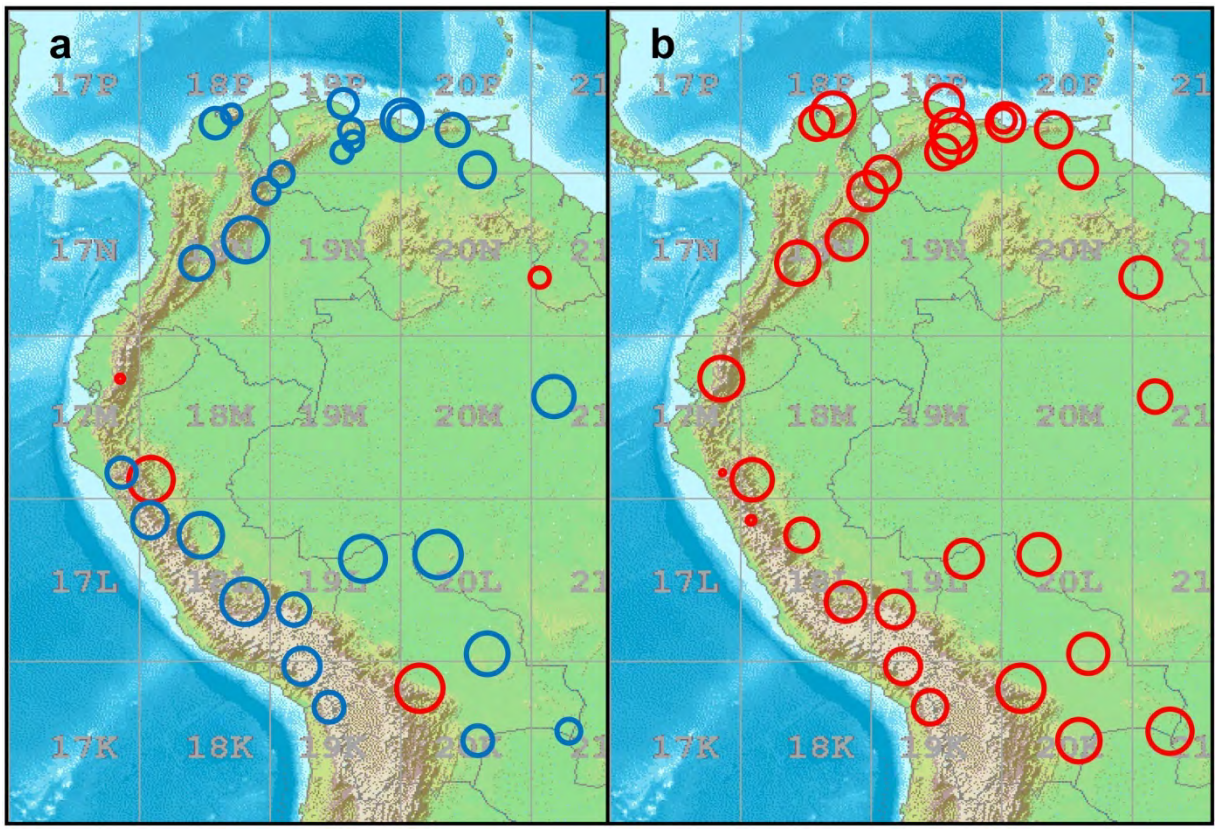

Supplementary Figure S6 | Correlations between yearly averages of diurnal temperature range (DTR) and minimum (T_{min}) or maximum (T_{max}) daily temperature throughout the northwestern South America. a, Mostly negative correlations between T_{min} and DTR (red circles: $r > 0$; blue circles: $r < 0$). b, All positive correlations between T_{max} and DTR. Circle size indicates the strength of the correlation between the two parameters at each location. Correlation coefficients and sample sizes (number of years of data at each site) are provided in Supplementary Table 8. This image of South America, which shows the latitude and longitude zones of the Universal Transverse Mercator coordinate system, was obtained from the Wikipedia Commons (http://upload.wikimedia.org/wikipedia/commons/9/9b/LA2-South-America-UTM-zones.png).

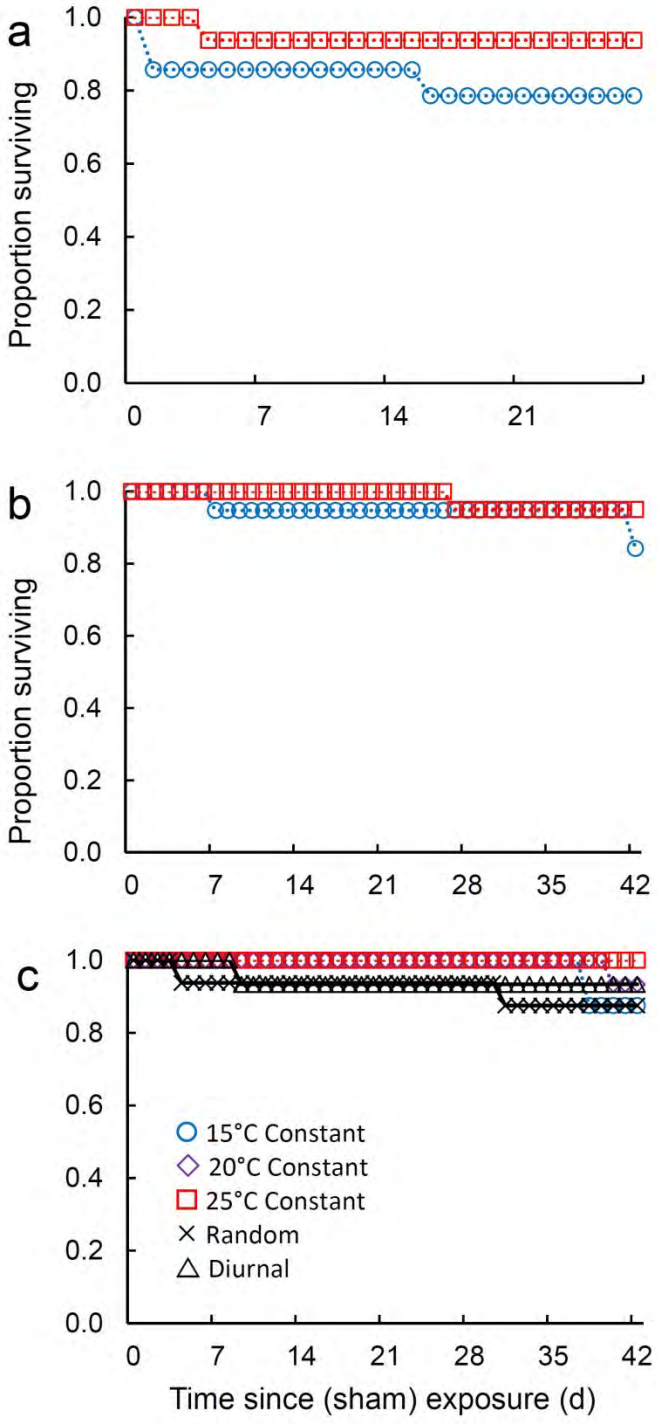

Supplementary Figure S7 | Survival of control frogs in the three experiments. a-b, Survival of uninfected frogs at different exposure temperatures (○ 15°C; □ 25°C) in *Acclimation Experiment 1* (a) and *Acclimation Experiment 2* (b). c, Survival of uninfected frogs in the *Diurnal Temperature Experiment* with different temperature treatments (○ 15°C; ◇ 20°C; □ 25°C; × Random; △ Diurnal).

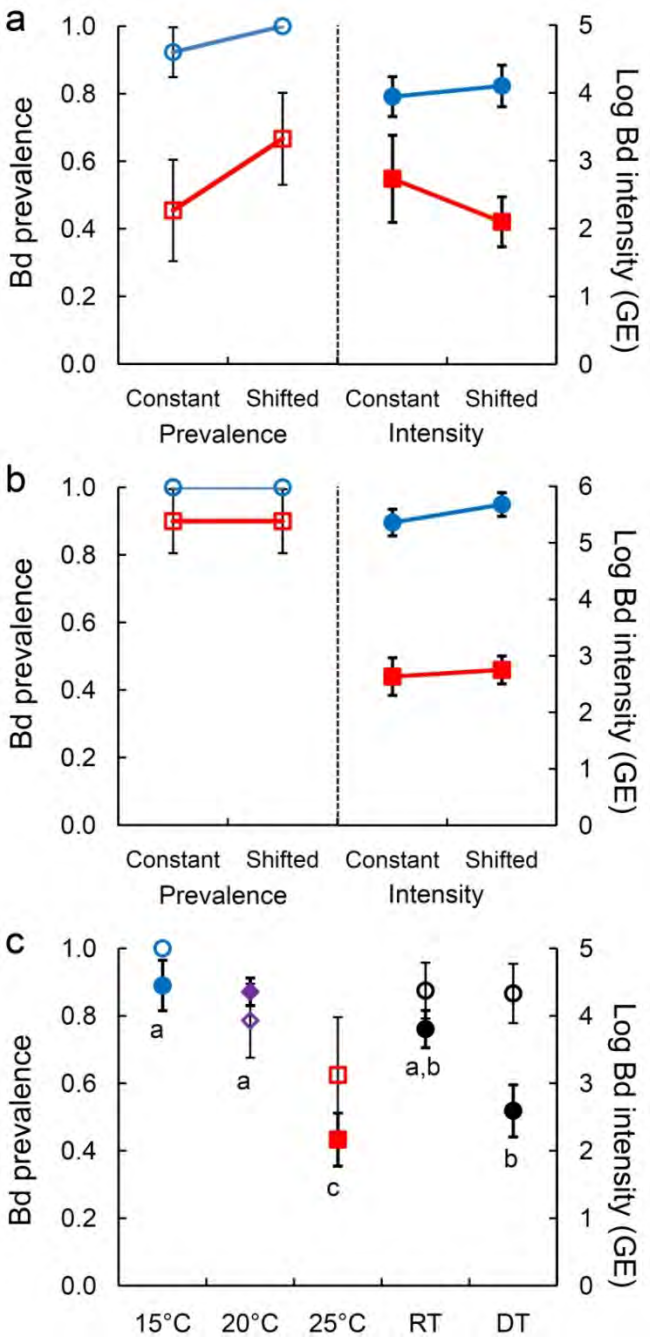

Supplementary Figure S8 | Effects of temperature treatments on *Batrachochytrium dendrobatidis* **(*Bd*) infection four weeks post-exposure in the three experiments.** a-b, Prevalence (open symbols) and log intensity (filled symbols) of infection for *Bd*-exposed frogs four weeks post-exposure for *Acclimation Experiment 1* (a) and *Acclimation Experiment 2* (b), including swabs of dead frogs surviving at least 23 days post-exposure (○ 15°C, □ 25°C). c, Prevalence and intensity of infection for the *Diurnal Temperature Experiment*. *Bd* intensity (zoospore genome equivalents, GE) excludes frogs with no measurable infection. Treatments labeled with the same letter were not significantly different from each other. Data points represent means ± SE.

Supplementary Table S1. Occurrence of > 5°C temperature shifts at daily, weekly, and monthly timescales in the Tampa Bay area (Florida) from 1995 to 2011. Weekly and monthly averages were calculated starting from 1/1/1995, and temperature shifts were calculated as the difference between adjacent days, weeks, or months. Average daily temperature data were obtained from the UD/EPA Average Daily Temperature Archive for Tampa/St. Petersburg (http://academic.udayton.edu/kissock/http/Weather/gsod95-current/FLTAMPA.txt; download 3/13/2012), compiled by J. K. Kissock (Department of Mechanical and Aerospace Engineering, University of Dayton).

Timescale	Sample size	Maximum increase	Maximum drop	> 5°C increases*	> 5°C drops*	> 7°C increases*	> 7°C drops*
Daily	6241	8.7 °C	-12.2°C	72	160	9	56
Weekly	838	9.3°C	-11.7°C	23	39	8	16
Monthly	205	7.3°C	-8.7°C	4	6	1	2

*Number of times temperature shifts of this magnitude occurred in 1995-2011

Supplementary Table S2. Results of analyses of *Batrachochytrium dendrobatidis* load (zoospore equivalents, measured by real-time PCR) for Week 2 and Week 4 of the *Acclimation* and *Diurnal Temperature Experiments*. The Week 2 (14 days) analyses included only swabs from frogs alive on day 14 and omitted swabs of dead frogs. The Week 4 analyses included swabs of dead frogs surviving at least until day 23. Bold type indicates significant differences. All analyses controlled for potential effects of the temporal or spatial blocks that were incorporated into the designs of the *Acclimation* and *Diurnal Temperature* experiments, respectively.

Experiment	Period	Predictor	Coef*	X^2	df	P
Acclimation expt 1	Week 2	**Temporal block**	**-2.81**	**4.2**	**1**	**0.041**
	(N = 57)	**Mass**	**2.38**	**8.5**	**1**	**0.003**
		Temperature	**-2.27**	**7.3**	**1**	**0.007**
		Acclimation	**-2.64**	**9.8**	**1**	**0.002**
		Temperature × Acclimation	2.24	0.7	1	0.418
	Week 4	**Temporal block**	**-2.92**	**4.0**	**1**	**0.044**
	(N = 47)	Mass	0.94	1.1	1	0.305
		Temperature	**-6.57**	**18.3**	**1**	**< 0.001**
		Acclimation	0.21	0.8	1	0.812
		Temperature × Acclimation	2.46	0.1	1	0.105
Acclimation expt 2	Week 2	Temporal block	0.06	< 0.1	1	0.912
	(N = 38)	Mass	1.07	0.7	1	0.393
		Temperature	**-4.20**	**22.9**	**1**	**< 0.001**
		Acclimation	-0.94	1.0	1	0.317
		Temperature × Acclimation	**3.86**	**13.0**	**1**	**< 0.001**
	Week 4	Temporal block	0.40	0.4	1	0.537
	(N = 36)	Mass	2.16	1.4	1	0.237
		Temperature	**-4.70**	**31.8**	**1**	**< 0.001**
		Acclimation	0.39	0.4	1	0.533
		Temperature × Acclimation	2.61	0.2	1	0.166
Diurnal temp expt	Week 2	**Spatial block**	**NA**	**32.8**	**7**	**< 0.001**
	(N = 61)	Mass	-0.52	3.0	1	0.081
		Treatment	**NA**	**20.3**	**4**	**< 0.001**
	Week 4	Spatial block	NA	5.4	7	0.610
	(N = 61)	**Mass**	**< 0.01**	**< 0.1**	**1**	**0.993**
		Treatment	**NA**	**10.7**	**4**	**0.030**

*coefficients, unstandardized

Supplementary Table S3. Results of separate analyses of *Batrachochytrium dendrobatidis* load (zoospore equivalents, measured by real-time PCR) for the 15°C and 25°C exposure temperature treatments of the *Acclimation experiments*. The frogs from each exposure temperature were analyzed separately to test for main effects of frog acclimation on *Bd* load, to aid in the interpretation of the main and interaction effects from the full models (Supplementary Table 2). These analyses included only swabs from frogs alive on Week 2, which are more straightforward to interpret than the Week 4 data because most frogs were still alive at this time point. All analyses controlled for potential effects of the temporal blocks that were incorporated into the *Acclimation* experiments. Bold type indicates significant differences.

Experiment	Exposure temperature	Predictor	Coef*	X^2	df	P
Acclimation expt 1	15°C (N = 29)	Temporal block	-1.00	1.5	1	0.222
		Mass	1.35	3.3	1	0.070
		Acclimation	**-2.26**	**6.5**	**1**	**0.011**
	25°C (N = 28)	**Temporal block**	**-10.23**	**5.8**	**1**	**0.016**
		Mass	2.26	3.5	1	0.061
		Acclimation	5.71	3.0	1	0.081
Acclimation expt 2	15°C (N = 19)	Temporal block	-0.77	0.8	1	0.386
		Acclimation	**-2.25**	**6.5**	**1**	**0.011**
	25°C (N = 19)	Temporal block	0.769	2.1	1	0.150
		Acclimation	0.736	2.3	1	0.127

*coefficients, unstandardized

Supplementary Table S4. Results of the overall frog survival analyses for the *Acclimation* and *Diurnal Temperature* experiments, including both *Batrachochytrium dendrobatidis* (*Bd*) exposed and control frogs. Survival was analyzed using survival regression (extreme value distribution), censoring frogs that survived until the end of each experiment. Significant treatment effects are highlighted in bold text, and sample sizes are indicated in parentheses. Positive coefficients indicate positive effects of predictors on frog survival. All analyses controlled for potential effects of the temporal or spatial blocks that were incorporated into the designs of the *Acclimation* and *Diurnal Temperature* experiments, respectively.

	Predictor	Coef*	X^2	df	P
Acclimation	**Temporal block**	**-4.20**	**9.9**	**1**	**0.002**
Expt 1 (N = 98)	**Mass**	**-0.48**	**24.6**	**1**	**< 0.001**
	***Bd*-exposure**	**-12.00**	**34.1**	**1**	**< 0.001**
	Temperature (warm)	**6.91**	**24.3**	**1**	**< 0.001**
	Acclimation	0.16	< 0.1	1	0.901
	Bd-exposure × Temperature	5.18	0.5	1	0.464
	Bd-exposure × Acclimation	-1.49	< 0.1	1	0.833
	Temperature × Acclimation	-1.94	0.4	1	0.523
	Bd-exposure × Temperature × Acclimation	-123.18	1.1	1	0.288
Acclimation	Temporal block	0.47	< 0.1	1	0.889
Expt 2 (N = 79)	Mass	3.66	0.3	1	0.562
	***Bd*-exposure**	**-23.69**	**44.4**	**1**	**< 0.001**
	Temperature (warm)	**27.61**	**49.7**	**1**	**< 0.001**
	Acclimation	**5.96**	**4.2**	**1**	**0.041**
	***Bd*-exposure × Temperature**	**26.67**	**5.2**	**1**	**0.022**
	Bd-exposure × Acclimation	**-0.93**	< 0.1	1	0.918
	Temperature × Acclimation	**-6.40**	0.4	1	0.527
	Bd-exposure × Temperature × Acclimation	**-194.1**	3.2	1	0.072
Diurnal Temp	Spatial block	NA	16.6	7	0.020
Expt (N = 126)	**Mass**	**0.24**	**21.8**	**1**	**< 0.001**
	***Bd*-exposure**	**-22.68**	**62.3**	**1**	**< 0.001**
	Treatment (temperature)	**NA**	**35.1**	**4**	**< 0.001**
	Bd-exposure × Treatment	NA	3.43	4	0.489

*coefficients, unstandardized

Supplementary Table S5. Results of the frog survival analyses for the *Acclimation* and *Diurnal Temperature Experiments*, including only *Batrachochytrium dendrobatidis* (*Bd*) exposed frogs. Survival was analyzed using survival regression (extreme value distribution), censoring frogs that survived until the end of each experiment. Significant treatment effects are highlighted in bold text, and sample sizes are indicated in parentheses. Positive coefficients indicate positive effects of predictors on frog survival. All analyses controlled for potential effects of the temporal or spatial blocks that were incorporated into the designs of the *Acclimation* and *Diurnal Temperature* experiments, respectively.

	Predictor	Coef*	X^2	df	P
Acclimation Expt 1 (N = 68)	**Temporal block**	**-4.31**	**12.6**	**1**	**< 0.001**
	Mass	-1.19	1.9	1	0.167
	Temperature (warm)	**6.60**	**23.8**	**1**	**< 0.001**
	Acclimation	-0.20	< 0.1	1	0.906
	Temperature × Acclimation	2.75	1.6	1	0.205
Acclimation Expt 2 (N = 40)	Temporal block	2.30	0.5	1	0.496
	Mass	2.46	0.2	1	0.688
	Temperature (warm)	**28.69**	**56.4**	**1**	**< 0.001**
	Acclimation	**6.99**	**5.9**	**1**	**0.015**
	Temperature × Acclimation	-91.50	3.2	1	0.075
Diurnal Temp Expt (N = 64)	**Spatial block**	**NA**	**21.5**	**7**	**0.003**
	Mass	0.26	2.4	1	0.121
	Treatment (temperature)	**NA**	**41.1**	**4**	**< 0.001**

*coefficients, unstandardized

Supplementary Table S6. Results of the *Atelopus* dataset reanalysis comparing and contrasting the predictive power of overall monthly temperature variability (Absolute value of monthly differences, AVMD[6]) with either monthly increases or decreases in temperature analyzed separately. The extinction dataset (1980-1998) included the proportion of species in the genus *Atelopus* that were last observed in each year (Last year observed, LYO) and the proportion of populations that were observed to decline each year (Year of decline, YOD)[6]. AVMD and DTR (Diurnal temperature range) were the best predictors of LYO and YOD in a previous study, with a 1-year lag for the effect of AVMD on LYO[6]. Response variables were detrended using generalized additive models (GAM) to control for temporal confoundment[6]. As in the original study, models were run with and without DTR as a covariate, and with or without detrending DTR[6]. Lower AIC_c values (e.g., more negative) indicate better models.

			AVMD			Monthly decreases			Monthly increases		
Response	Covariate	df	AIC_c	*F*	*P*	AIC_c	*F*	*P*	AIC_c	*F*	*P*
LYO*†	None	1,17	-37.8	7.2	**0.016**	-35.8	4.8	**0.042**	-35.2	4.1	0.059
YOD*	None	1,17	-24.8	0.1	0.897	-24.9	0.2	0.677	-25.3	0.5	0.493
LYO*†	DTR*†	1,16	-45.9	18.6	< **0.001**	-42.5	13.0	**0.002**	-39.3	8.5	**0.010**
YOD*	DTR*†	1,16	-39.1	3.7	0.072	-40.6	5.4	**0.034**	-35.3	0.1	0.718
LYO*†	DTR†	1,16	-49.1	29.0	< **0.001**	-47.9	26.1	< **0.001**	-37.5	8.4	**0.010**
YOD*	DTR†	1,16	-35.6	4.9	**0.043**	-39.2	9.2	**0.008**	-30.6	0.1	0.885

*Detrended using GAM [6]

†Analyzed with a one-year lag between predictor and response [6]

Supplementary Table S7. Effects of temperature on *Batrachochytrium dendrobatidis* growth in culture (proportional increase in zoosporangia over 7 days), analyzed using a generalized linear model with gamma-distributed errors. Blocking factors were included to control for potential effects of the temporal or spatial blocks of the *Acclimation* and *Diurnal Temperature* experiments, respectively.

	Predictor	X^2	df	P
Acclimation Expt 1 (N = 80)	Temporal block	1.4	1	0.231
	Exposure temperature	**86.3**	**1**	**< 0.001**
Diurnal Temp Expt (N = 64)	**Spatial block**	**6.7**	**7**	**0.443**
	Treatment	**72.0**	**4**	**< 0.001**

Supplementary Table S8. South American climate datasets used to assess relationships between average daily minimum temperature (T_{min}), daily maximum temperature (T_{max}) and diurnal temperature range (DTR) for the years 1980-2004. The station code, name, and location are listed for each dataset, as well as the number of years sampled. Correlation coefficients (r) are listed for the relationships between T_{min} and DTR and between T_{max} and DTR.

Code	Station (Country)	Lat.	Long.	N[†]	$r_{Tmin/DTR}$	$r_{Tmax/DTR}$	DTR range[‡]
800220	Cartagena/Rafael Nu (CO)	10.45°	-75.52°	25	-0.329	0.464	4.8 – 6.1
800280	Barranquilla/Ernest (CO)	10.88°	-74.78°	25	-0.134	0.793	6.7 – 8.7
800940	Bucaramanga/Paloneg (CO)	7.10°	-73.20°	21	-0.238	0.614	5.9 – 7.3
800970	Cucuta/Camilo Daza (CO)	7.93°	-72.52°	15	-0.217	0.520	7.9 – 9.4
802220	Bogota/Eldorado (CO)	4.70°	-74.15°	25	-0.739	0.681	10.0 – 13.3
802590	Cali/Alfonso Bonill (CO)	3.55°	-76.38°	25	-0.402	0.775	9.6 – 11.4
804030	Coro (VE)	11.42°	-69.68°	23	-0.299	0.579	6.6 – 8.5
804100	Barquisimeto (VE)	10.07°	-69.32°	24	-0.211	0.778	8.4 – 10.8
804150	Caracas/Maiquetia A (VE)	10.60°	-66.98°	25	-0.611	0.246	5.6 – 8.2
804160	Caracas/La Carlota (VE)	10.50°	-66.88°	22	-0.385	0.588	6.9 – 10.5
804190	Barcelona (VE)	10.12°	-64.68°	24	-0.367	0.512	6.9 – 10.0
804270	Acarigua (VE)	9.55°	-69.23°	22	-0.137	0.781	7.9 – 11.0
804280	Guanare (VE)	9.02°	-69.73°	24	-0.156	0.479	9.4 – 10.6
804440	Ciudad Bolivar (VE)	8.15°	-63.55°	19	-0.442	0.564	7.7 – 10.0
820220	Boa Vista Aeroport (BR)	2.83°	-60.70°	23	0.010	0.689	7.6 – 9.3
821110	Eduardo Gomes Intl (BR)	-3.03°	-60.05°	25	-0.611	0.429	7.5 – 9.5
842030	Guayaquil Aeropuert (EC)	-2.15°	-79.88°	25	0.001	0.793	6.1 – 9.4
844520	Chiclayo (PE)	-6.78°	-79.82°	25	-0.324	0.007	8.0 – 9.6
844720	Cajamarca (PE)	-7.13°	-78.47°	17	0.054	0.710	13.1 – 15.8
845310	Chimbote (PE)	-9.13°	-78.52°	17	-0.462	0.026	6.0 – 9.9
845640	Huanuco (PE)	-9.87°	-76.20°	20	-0.718	0.451	10.8 – 14.1
846730	Ayacucho (PE)	-13.15°	-74.20°	17	-0.787	0.650	12.4 – 18.2
846860	Cuzco (PE)	-13.53°	-71.93°	25	-0.371	0.579	14.1 – 16.9
847520	Arequipa (PE)	-16.33°	-71.57°	25	-0.500	0.532	13.3 – 15.3
850330	Guayaramerin (BO)	-10.82°	-65.35°	19	-0.809	0.696	9.3 – 13.3
850410	Cobija (BO)	-11.03°	-68.78°	22	-0.762	0.598	9.0 – 11.7
851750	Ascencion De Guaray (BO)	-15.72°	-63.10°	17	-0.659	0.667	9.2 – 12.6
852230	Cochabamba (BO)	-17.42°	-66.18°	25	0.058	0.928	16.4 – 19.5
853150	Camiri (BO)	-20.00°	-63.53°	20	-0.333	0.780	9.6 – 13.5
854060	Arica (CL)	-18.35°	-70.33°	25	-0.336	0.491	4.6 – 7.4
860110	Base 5 Gral A.Jara (PY)	-19.53°	-59.37°	20	-0.215	0.848	8.0–13.7

[†]Sample size, i.e., the number of years in 1980-2004 with at least 150 days of complete data
[‡]Minimum and maximum of the mean annual DTR for the years 1980-2004

Supplementary Table S9. Packages and functions used in statistical analyses (R statistical software).

Analysis	Package	Function
Cox proportional hazards regression	Survival[39]	survreg()
Generalized linear model (glzm), gamma or Gaussian errors	Base[31]	glm()
Likelihood-ratio tests for glm(), type = "II"	Car[40]	Anova()
Likelihood-ratio tests for survreg()	Base[31]	drop1()
Likelihood-ratio tests for zeroinfl()	Lmtest[41]	lrtest()
P-value corrections for multiple comparisons	Multtest[42]	mt.rawp2adjp()
Zero-inflated generalized linear model, dist="negbin"	Pscl[34,43]	zeroinfl()
Path analysis	Lavaan[44]	sem